Transport of silver nanoparticles from nanocomposite Ag/alginate hydrogels under conditions mimicking tissue implantation

Danijela D. Kostic[1], Ivana S. Malagurski[2], Bojana M. Obradovic[2]

[1]*Innovation Center of the Faculty of Technology and Metallurgy, Belgrade, Serbia*
[2] *Faculty of Technology and Metallurgy, University of Belgrade, Belgrade, Serbia*

Abstract

The aim of this work was to assess phenomena occurring during AgNP transport from nanocomposite Ag/alginate hydrogels under conditions relevant for potential biomedical applications as antimicrobial soft tissue implants. First, we have studied AgNP migration from the nanocomposite to the adjacent alginate hydrogel mimicking soft tissue next to the implant. AgNP deposition was carried out by the initial burst release lasting for ~24 h yielding large aggregates on hydrogel surfaces and smaller clusters (~400 nm in size) inside. However, the overall released content was low (0.67%) indicating high nanocomposite stability. In the next experimental series, release of AgNPs, 10–30 nm in size, from Ag/alginate microbeads in water was investigated under static conditions as well as under continuous perfusion mimicking vascularized tissues. Mathematical modeling has revealed AgNP release by diffusion under static conditions with the diffusion coefficient within the Ag/alginate hydrogel of 6.9×10^{-19} m^2 s^{-1}. Conversely, continuous perfusion induced increased AgNP release by convection with the interstitial fluid velocity estimated as 4.6 nm s^{-1}. Overall, the obtained results indicated the influence of hydrodynamic conditions at the implantation site on silver release and potential implant functionality, which should be investigated at the experimentation beginning using appropriate *in vitro* systems.

Keywords: silver nanoparticles, aggregation, convection, mathematical modeling, tissue implants.

Available online at the Journal website: http://www.ache.org.rs/HI/

Silver is known for centuries to exhibit strong antimicrobial activity but it has attracted renewed attention for use in medicine and healthcare as the advancements in nanotechnology provided different methods for production of this metal in the nanoparticle form [1–3]. Silver nanoparticles (AgNPs) have been reported to be more potent than silver ions [4] and could be embedded into polymer matrices providing extended functionality of different medical and healthcare products [2]. Enrichment of polymer hydrogels with antimicrobial properties is especially desirable for wound dressings [4–6] but also for tissue implants in order to prevent infections and biofilm formation [7]. Alginate hydrogels are commonly used in wound dressings due to excellent biocompatibility and high sorption capacity providing regulation of moisture levels in the wound [8]. Due to hydrophilicity and structural resemblance to soft tissues these hydrogels are also widely investigated for tissue engineering applications [9] such as tissue engineering of intervertebral discs [10] as well as cartilage [11,12]. However, alginate hydrogels play a

fairly passive role in the body and thus, there are numerous approaches to extend the functionality such as the addition of different bioactive agents including ionic silver and AgNPs [9]. One of the routes to produce nanocomposite Ag/alginate hydrogels is the electrochemical synthesis of AgNPs in alginate solutions followed by gelation of the obtained colloids [13,14]. This method provides the use of just several chemicals and hydrogel products that contain only Ca-alginate and AgNPs [13]. However, medical applications of nanocomposites require comprehensive studies of biocompatibility, interactions with biological fluids, cytotoxicity and genotoxicity including the fate of nanoparticles in the body [15]. Nanoparticles in general, can be transported internally to different organs, tissues and cells by diffusion as well as by the blood flow accompanied by various complex phenomena such as aggregation and flocculation, hindered behavior of particles in confined spaces, binding, and retention at specific sites [16]. For example, upon the intraperitoneal injection in rats, AgNPs were reported to be carried by the mesenteric vein and distributed into hepatic tissues via the portal system [17]. Also, after repeated intraperitoneal injections in rats, AgNPs were found in spleen and kidneys [18]. Similarly, it is suggested that AgNPs can pass through dermal and lung barriers as well as through the gastrointestinal tract into the blood resulting in nanoparticle distribution within the body after pulmonary,

dermal and oral exposures [19]. In addition, AgNPs were observed to form aggregates within cells and tissues when administered intraperitonealy [17,18] as well as when applied in wound dressings [20]. This finding is particularly important as the nanoparticle size influences many of the mentioned processes in the body such as the diffusion rate, adsorption of proteins and consequently particle stability, uptake by cells and attachment to endothelial surfaces [16,21]. Larger nanoparticles were reported to be less toxic than the smaller ones [22] as well as more easily recognized by macrophages resulting in lower distribution throughout the body [19].

Thus, development and utilization of novel nanocomposite materials in biomedical applications requires the knowledge of mechanisms and kinetics of release of silver nanoparticles and/or ions in order to provide desired antimicrobial functionality as well as to predict the fate of nanoparticles in the body and avoid any potential adverse effects. In this respect, hydrogels, apart from being beneficial, biocompatible biomaterials are also suitable for studies of nanoparticle interactions and transport within the matrices, which bear resemblance to certain *in vivo* settings as many tissues and sites are gel-like in nature [23].

We have previously developed mathematical models that describe silver release from Ag/alginate hydrogels in water as well as in the presence of chloride ions in physiological saline solution [24]. The diffusion coefficient of AgNPs 4 nm in diameter in Ag/alginate hydrogel (1.73%) produced using medium viscosity alginate was estimated as 1.27×10^{-18} m^2 s^{-1} [24]. In the present study, we have further investigated phenomena occurring during AgNP diffusion from Ag/alginate hydrogels in water under conditions relevant for hydrogel implantation. First, we have investigated if the AgNPs could diffuse intact into a hydrogel in direct contact with the nanocomposite mimicking nanocomposite implantation in a soft tissue site. Next, we have investigated application of the same diffusion model to the release of larger AgNPs (10–30 nm in diameter) from Ag/alginate hydrogel microbeads produced by using low viscosity alginate. By lowering the viscosity of alginate it is possible to reduce the size of the resulting Ca-alginate microbeads produced by electrostatic droplet generation technique [25], which was used in the present study. Furthermore, the effect of alginate viscosity on the microbead size is similar in other production methods such as vibrating nozzle technology [26], which was also reported to be limited to low alginate viscosities up to 0.2 Pa s [27]. Similar limitations by the fluid viscosity were reported for most of the production techniques of polymer microbeads with the exception of jet cutting method [28]. This technique can be applied to polymer solutions of low as well as

high viscosities with the note that higher viscosities result in higher pressure drops in the nozzles, which can be overcome by modification of the experimental apparatus [28]. Finally, we have also investigated silver release from the nanocomposite microbeads in a perfused packed bed bioreactor relevant for nanocomposite implantation in a vascularized tissue site.

EXPERIMENTAL

Materials

Medium viscosity sodium alginate (A 2033) and low viscosity sodium alginate (A 2158) were supplied from Sigma (St. Louis, MO). AgNO$_3$ was purchased from M. P. Hemija (Belgrade, Serbia), KNO$_3$ and Ca(NO$_3$)$_2$·4H$_2$O from Centrohem (Stara Pazova, Serbia), citrate dihydrate (W302600) from Sigma (St. Louis, MO), nitric acid (65%) from ZorkaPharma (Šabac, Serbia), and ammonium hydroxide (25%) from NRK Inženjering (Belgrade, Serbia). Water from Milli-Q system (Millipore, Billerica, MA) was used in all experiments and N$_2$ gas was of high purity (99.5%).

Production of Ag/alginate colloid solutions

AgNPs stabilized by alginate were produced by electrochemical synthesis using aqueous solutions containing 0.1 M KNO$_3$, 2% Na-alginate, and 3.9 mM AgNO$_3$, as described previously [13,14]. Electrochemical synthesis was performed galvanostatically under continuous stirring at the current density of 50 mA cm^{-2} and during the implementation time of 10 min in an electrochemical cell containing two Pt electrodes, and a reference, saturated calomel electrode (SCE) using Gamry Reference 600 Potentiostat/Galvanostat/ZRA (Gamry Instruments, Warminster, PA). The solution was exposed to N$_2$ for 20 min prior the synthesis, as well as during the synthesis. Final alginate concentrations were 1.9 and 1.73% for low and medium viscosity alginate, respectively, due to slight alginate gelation and deposition on the electrode during the synthesis, as described previously [13]. Low viscosity alginate colloid solutions with 1 mM AgNP concentration were obtained by diluting the initially synthesized colloid solutions with 1.9% Na-alginate solution.

Production of Ag/alginate discs

Ag/alginate discs were produced by pouring the initially synthesized medium viscosity 3.9 mM Ag/alginate colloid solution (20 cm^3) into a Petri dish (8 cm in diameter) covered by a filter paper (0.2 μm pore diameter, 90 mm in diameter; Pall membrane filters, Sigma Aldrich, USA) saturated in the gelling solution containing 1.5% Ca(NO$_3$)$_2$×4H$_2$O. The solution was covered by another filter paper over which 30–40 cm^3 of the gelling solution was slowly transferred. After 48

h, the filter papers were removed and the obtained Ag/alginate hydrogel was left in the gelling solution for another 48 h. Discs (2 cm in diameter, 2 mm thick) were then cored out using a metal ring and left for 24 h in the gelling solution to complete gelation. Discs were finally thoroughly rinsed in distilled water in order to remove residual ions. Control alginate discs were produced using the same procedure and 1.73% medium viscosity alginate solution.

Silver diffusion into alginate discs

Silver transport from the obtained Ag/alginate discs with the nominal silver concentration of 3.9 mM into pure alginate discs was investigated under static conditions in 6 well plates. Each well contained an alginate disc on top of which an Ag/alginate disc was placed and pressed by a piece of rubber attached to the plate cover (Fig. 1a). In such a way, movement of the discs was prevented and each well was filled with 10 cm^3 of distilled water. The experiment was performed at room temperature (~25 °C) in dark under atmospheric conditions in triplicate for each time point and lasted for up to 14 days. For each time point, experimental systems were emptied and the discs were analyzed regarding the presence of AgNPs and the total silver content.

Production of Ag/alginate microbeads

Alginate microbeads containing AgNPs were prepared using diluted low viscosity Ag/alginate colloid solutions and electrostatic droplet generation as described previously [13]. In brief, 1 mM Ag/alginate colloid solution was extruded by a syringe pump through a positively charged blunt edge stainless steel needle (25 gauge, 7 kV applied electrostatic potential) positioned at a distance of 2 cm between the needle tip and the grounded gelling bath (1.5 % w/v Ca(NO$_3$)$_2$ x 4H$_2$O). The resulting microbeads were left in the gelling

bath for additional 30 min in order to complete gelling, followed by washing 2 times in distilled water.

Silver release from Ag/alginate microbeads

Silver release from 1 mM Ag/alginate microbeads was investigated under static conditions and continuous perfusion using 4 g (with the accuracy of 1 mg) of microbeads in 10 cm^3 of distilled water in each experimental set-up. Static experiments were performed in Petri dishes (8 cm in diameter) providing a monolayer of microbeads while continuous perfusion experiments were carried out in packed bed bioreactors (Fig. 1b). Perfusion bioreactors consisted of two glass parts, fitted into a piece of silicone tubing 9 mm in diameter and 9 cm long so that the total volume of the bioreactor chamber was 5.7 cm^3. Built-in sintered glass plates prevented outflow of microbeads from the chamber. Each bioreactor was connected to a separate recirculation loop consisting of a water reservoir, silicone tubing and two syringes for removal of gas bubbles. Water flow rate trough the bioreactor packed with Ag/alginate microbeads was 0.4 cm^3 min^{-1}. All experiments were performed at 37±0.1 °C in dark under atmospheric conditions in triplicate for each time point and lasted up to 21 days. For each time point, experimental systems were emptied and analyzed regarding the presence of AgNPs in microbeads by UV–Vis spectroscopy as well as the total silver concentration in water.

Analytical methods

UV–Vis spectroscopy

Presence of AgNPs in nanocomposite microbeads and discs was examined by the UV-3100 spectrophotometer (Shanghai MAPADA Instruments, China) after dissolution in 2% sodium citrate solution (0.1 g of microbeads or discs in 2.9 cm^3 of the solution).
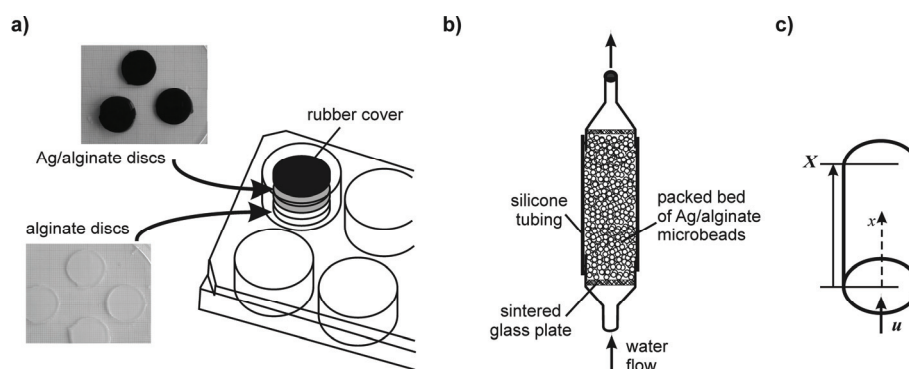

Figure 1. Experimental set-up for silver release studies. a) Ag/alginate discs: in each well of a 6-well plate an alginate disc was placed on top of which an Ag/alginate disc was positioned and pressed by a piece of rubber attached to the plate cover; 10 cm^3 of distilled water was added to each well. b) Packed bed bioreactor: two glass pieces with sintered glass plates at the ends were fitted into a piece of silicone tubing filled with Ag/alginate microbeads. c) Hydrogel geometry used for mathematical modeling of silver release from the packed bed of Ag/alginate microbeads by diffusion and convection in axial direction, x; X is the length of the cylindrical hydrogel and u is the interstitial fluid velocity through the hydrogel.

Measurement of silver concentration

Silver content in Ag/alginate microbeads was determined upon oxidation of all AgNPs by addition of concentrated nitric acid (65%) in excess (5 cm^3 of the acid per 0.1 g of microbeads). Silver content in Ag/alginate discs was determined by dissolving the discs in 10% sodium citrate solution (0.5–0.8 g in 5 cm^{3}of the solution) followed by oxidation of all AgNPs by addition of ammonium hydroxide (20 cm^3 of the 25% NH$_4$OH per 0.5–0.8 g of discs). Silver content in alginate discs into which AgNPs/ions have diffused, was determined using the same procedure with slightly different ratios (*i.e.*, 0.5–0.8 g in 3 cm^3 of the citrate solution into which 3 cm^3 of the 25% NH$_4$OH solution was then added). Concentration of Ag$^+$ in all resulting solutions was then determined at three-digit accuracy by flame atomic absorption spectrometry (FAAS) using Perkin Elmer 3100 spectrometer (Perkin Elmer, AAnalyst 300, USA).

Optical microscopy

Microbead diameters were determined by using an optical microscope (Olympus CX41RF, Tokyo, Japan). The average diameter was calculated from measurements of at least 20 microbeads on slides in water using the image analysis program "CellA" (Olympus, Tokyo, Japan). Images of alginate disc surfaces were acquired directly.

Field-emission scanning electron microscopy (FE-SEM)

Cross-sections of Ag/alginate and alginate discs for FE-SEM analysis were obtained using a previously described procedure [29] that was slightly modified. In brief, discs were immersed sequentially in aqueous solutions containing 3% acetic acid, then 3% acetic acid and 25% ethanol, followed by 3% acetic acid and 50% ethanol, and finally the aqueous solution with 70% ethanol. Next, the discs were sliced into thin slices,

mounted onto microscope glass slides cut in pieces, dried and analyzed using MIRA 3 XMU Field Emission Scanning Electron Microscope (Tescan USA Inc., Cranberry Twp, PA).

EXPERIMENTAL RESULTS

The main goal of this work was to assess phenomena during transport of AgNPs from Ag/alginate hydrogels under conditions relevant for hydrogel implantation. In specific, we have investigated AgNP transport into alginate hydrogel as a tissue-like phase and into water as a fluid phase under static and fluid flow conditions.

AgNP/ion diffusion into alginate discs

Both Ag/alginate and alginate discs retained dimensions and weights during the 14 day experiment, which is expected due to stability of alginate hydrogels in water. The initial silver concentration in Ag/alginate disc was determined by FAAS as 6.2±1.3 mM, which is higher than the silver concentration in the initial Ag/ /alginate colloid solution (3.9 mM). This result indicates gel contraction during Ag/alginate gelation as previously reported for Ca/alginate hydrogels to be in the range 30–50% [30]. The final silver concentration after 14 days in Ag/alginate discs (6.4±0.2 mM) was not significantly different than the initial silver concentration while AgNPs within the Ag/alginate discs could be observed by FE-SEM analyses (Fig. 2a). However, optical microscopy (Supplementary material, available from the corresponding author on request) as well as FE--SEM analyses (Fig. 2b) have shown that over 14 days during the static experiment, a certain amount of AgNPs and/or silver ions has diffused into the alginate discs and formed nanoparticle aggregates. Yet, these aggregates could not be detected by UV–Vis spectro-
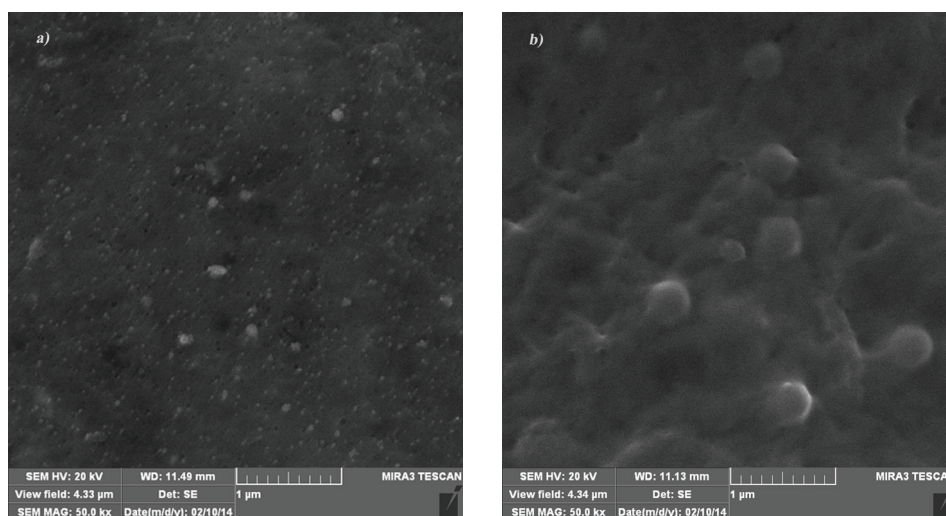

Figure 2. FE-SEM micrograph of the central part of the disc cross-section after 14 days of experiment: a) Ag/alginate disc; b) alginate disc beneath the Ag/alginate disc (scale bar = 1 µm).
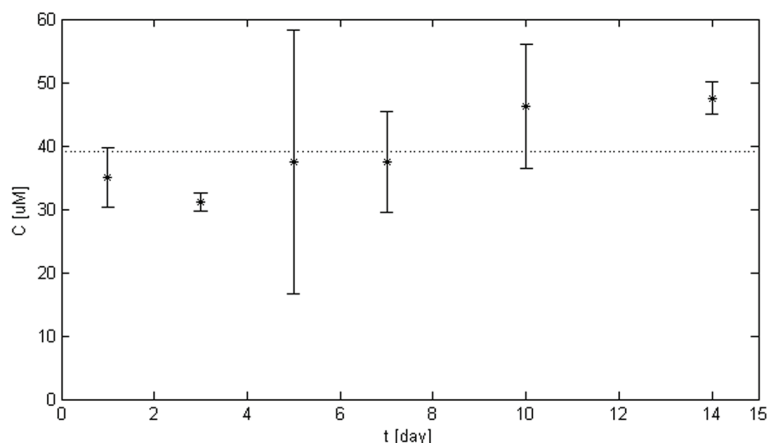
Figure 3. Silver concentration in alginate discs over time: experimental data (symbols) and the average value of 39 μM (dashed line) (data represent average of n = 3).

scopy. Still, by using FAAS total silver concentrations in alginate discs could be measured over time (Fig. 3). It could be noticed that the silver concentration quickly reached the value of ~35 μM determined after the first day of experiment and then negligibly increased over the next 13 days. These results imply that there was an initial burst release of AgNPs/ions probably from the surfaces of Ag/alginate discs. Thus, the average silver concentration in alginate discs over 14 days of experiment was 39±6 μM largely determined by the initial burst release.

Silver release from Ag/alginate microbeads

We have previously investigated silver release from Ag/alginate microbeads produced using medium viscosity alginate under static and well-mixed conditions in water. In the present study, we have applied the same modeling approach for silver release from Ag/alginate microbeads produced using low viscosity alginate, which contained AgNPs 10–30 nm in size [13]. Furthermore, we have investigated silver release from the microbeads under static conditions and in a packed bed continuously perfused by water relevant for hydrogel implantation in a vascularized site. The average microbead diameter was 590±60 μm while the initial silver concentration was determined by FAAS as 1.2±0.1 mM. It should be noted that we have assumed that during the electrochemical synthesis practically all of Ag^+ are reduced to AgNPs as adopted previously [24]. In brief, previous experimental characterization of electrochemical synthesis of AgNPs in alginate solutions has shown that the maximal absorbance in the UV–Vis spectrum, directly proportional to the AgNP concentration, reaches a plateau when the applied current density was increased above 25 mA cm^{-2} and at implementation times longer than 6 min [13]. In the present study, the current density of 50 mA cm^{-2} and the implementation time of 10 min were used implying complete reduction of Ag^+.

Silver release from Ag/alginate microbeads in water under static conditions was very low yielding the concentration of 6.1±0.7 μM measured after 21 days. This concentration in water corresponded to 1.3% of the initial AgNP content in microbeads. Additionally, AgNPs within microbeads in static conditions remained stable (Fig. 4a). On the other hand, under continuous perfusion silver release was significantly higher yielding the total silver concentration in water after 12 days of 38.8±0.7 μM. This concentration corresponds to 8.1%
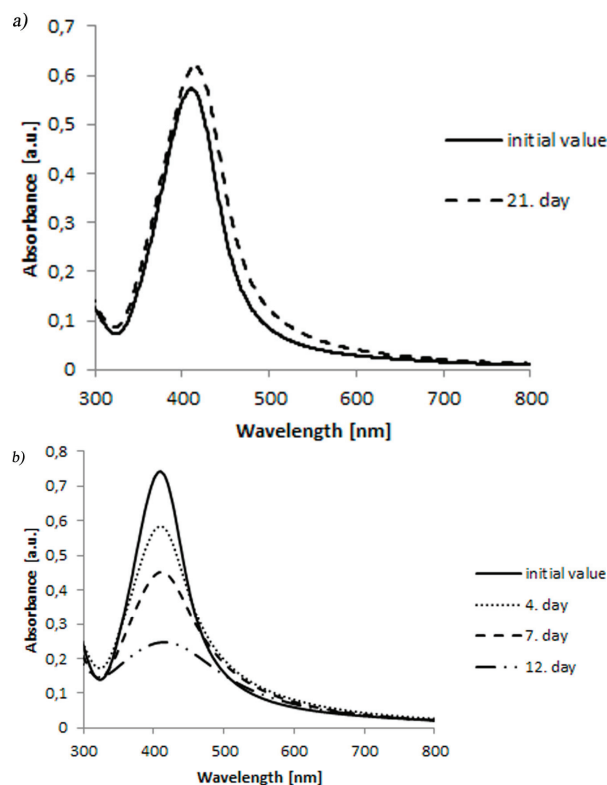

Figure 4. UV–Vis spectra of dissolved Ag/alginate microbeads over time: a) static conditions; b) continuously perfused packed bed (data represent average of n = 3).

of the initial AgNP content in microbeads. In addition, AgNPs within microbeads aggregated as observed visually as well as by UV-vis spectra, which became broad with decreased maximum absorbance value (Fig. 4b).

Mathematical modeling of silver release from Ag/alginate microbeads

Static conditions

In the present work, we have applied the same assumption as previously adopted [24] that silver release from Ag/alginate microbeads in water under static conditions was governed by AgNP diffusion within the alginate hydrogel. In addition, negligible microbead swelling was experimentally observed so that the constant microbead diameter of 590 μm was assumed. Thus, the governing equation for the temporal change in AgNP concentration in a spherical microbead, c_n, is:

$$\frac{\partial c_n}{\partial t} = D_n \left(\frac{\partial^2 c_n}{\partial r^2} + \frac{2 \partial c_n}{r \partial r} \right) \tag{1}$$

where D_n is the diffusion coefficient of AgNPs within the alginate gel matrix and r is the radial coordinate in the spherical microbead. It should be noted that under static conditions, D_n is the apparent diffusion coefficient including the external mass transfer through the liquid boundary. The rate of silver accumulation in surrounding water is equal to the silver release rate across the boundary, which in terms of the volume of microbeads, V, can be expressed as:

$$\frac{dc_m}{dt} = -\frac{3V}{RV_m} D_n \left(\frac{\partial c_n}{\partial r} \right)_{r=R} \tag{2}$$

where c_m is the total silver concentration in water, V_m is the water volume (10 cm³), and R is the microbead radius. Volume of the microbeads was calculated based on the microbead weight of 4 g and experimentally

determined microbead density of 1020±10 kg m⁻³ amounting to 3.9 cm³.

Initially, the AgNP distribution in microbeads is uniform at the initial concentration c_0, experimentally determined as 1.2 mM while AgNPs are not present in water. At the microbead surface the AgNP concentration is equal to that in the surrounding medium, which is assumed to be 0 as the released silver concentration in water was negligible as compared to that in the microbeads. Finally, in the microbead center, the symmetry condition was applied.

Eqs. (1) and (2) were solved numerically using MatLab based on the centered finite difference method for the second derivative of concentration and backward finite difference method for the first derivative of concentration. The AgNP diffusion coefficient, D_n, was determined by the least squares fit to the experimental data. Figure 5 presents experimental data and the best model predictions of silver concentrations in water over time showing satisfactory agreements (*STD* = = 17.4%). The AgNP diffusion coefficient within alginate microbeads was thus estimated as 6.9×10^{-19} m² s⁻¹.

Continuously perfused packed bed

Silver release from the packed bed of Ag/alginate microbeads continuously perfused by water was significantly higher than that under static conditions so that the same internal diffusion model could not describe the experimental results (application of the internal diffusion model in the integral form to the experimental data can be obtained from the corresponding author upon request). Based on the experimental results of increased silver release in this system while the AgNPs partially aggregated within the microbeads, we have supposed that AgNPs were actually washed out from the alginate hydrogel rather than oxidized. In order to estimate the convective transport through the hydrogel we have applied a simplified geometry of a
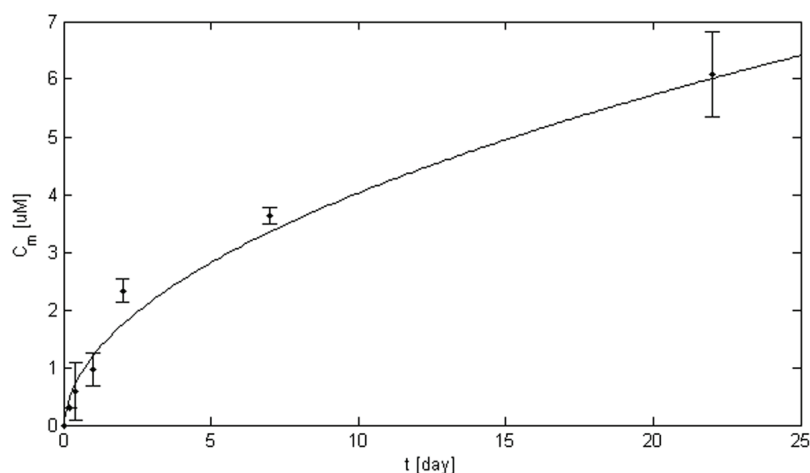

Figure 5. Released silver concentrations from Ag/alginate microbeads in water over time under static conditions: experimental data (symbols) and model predictions (lines); data represent average of n = 3.

hydrogel cylinder (Fig. 1c) formed by packed micro-beads from which AgNPs were released by diffusion as well as by the convective flow. The fluid flow and AgNP diffusion are assumed to be in the axial direction only.

Therefore, the temporal change in AgNP concentration in the cylinder formed of packed microbeads, c_n, is now expressed as the advection-diffusion equation:

$$\frac{\partial c_n}{\partial t} = D_n \frac{\partial^2 c_n}{\partial x^2} - u \frac{\partial c_n}{\partial x} \qquad (3)$$

where x is the axial coordinate and u is the velocity of water through the hydrogel. The released silver concentration in water over time is calculated as a difference between the initial silver content in the hydrogel and the silver content at each time point:

$$c_m = \frac{(c_0 - c_n)V}{V_m} \qquad (4)$$

where V is the hydrogel volume (3.9 cm^3), V_m is the water volume in the system (10 cm^3), while the average silver concentration in the hydrogel at each time point can be calculated by the equation:

$$\langle c_n \rangle = \frac{1}{X} \int_0^X c_n(x) \mathrm{d}x \qquad (5)$$

where X is the length of the cylindrical hydrogel (6.1 cm) comprising the volume of the microbeads (*i.e.*, 3.9 cm^3). The same initial condition of the uniform AgNP concentration in the hydrogel of 1.2 mM is assumed while the AgNP concentration at the hydrogel surface is equal to that in the surrounding water. However, based on the experimental measurements of total silver concentrations in water it could be assumed that the AgNP concentration in water could be neglected as compared

to that in the hydrogel. Thus, the AgNP concentration at the inlet cylinder boundary was set to be 0 while the Neumann boundary condition was set at the outlet boundary:

$$\frac{\partial c_n}{\partial x} = 0 \ \text{ for } x = X \qquad (6)$$

Eq. (3) was solved numerically using MatLab based on the backward finite difference method. The AgNP diffusion coefficient, D_n, was set to the value determined under static conditions, *i.e.*, $D_n = 6.9 \times 10^{-19}$ m^2 s^{-1}. Thus, the only adjustable parameter in this model was the internal fluid velocity through the hydrogel u determined by the least squares fit to the experimental data.

Figure 6 presents experimental data and the best model predictions of released silver concentrations under water flow in perfusion bioreactors together with the predictions of the internal diffusion model. It could be seen that the release by internal diffusion was low compared to the impact of fluid flow. Satisfactory agreements were obtained (*STD* = 24.8%) with the fluid velocity within the hydrogel estimated as 4.6×10^{-9} m s^{-1}. Compared to the experimental superficial fluid velocity in this system of about 1×10^{-4} m s^{-1}, the modeling results imply that only ~6×10^{-3}% of the fluid flowrate passes through the hydrogel.

In order to further evaluate the effects of model parameters, sensitivity analysis was performed by changing the parameter values for ±50% of the baseline values. The change in AgNP diffusion coefficient significantly affected AgNP release from Ag/alginate microbeads under static conditions (Fig. 7a) and negligibly under perfusion (Fig. 7b). Under fluid perfusion in the packed bed bioreactor the interstitial fluid velocity within the alginate hydrogel governed the silver release.
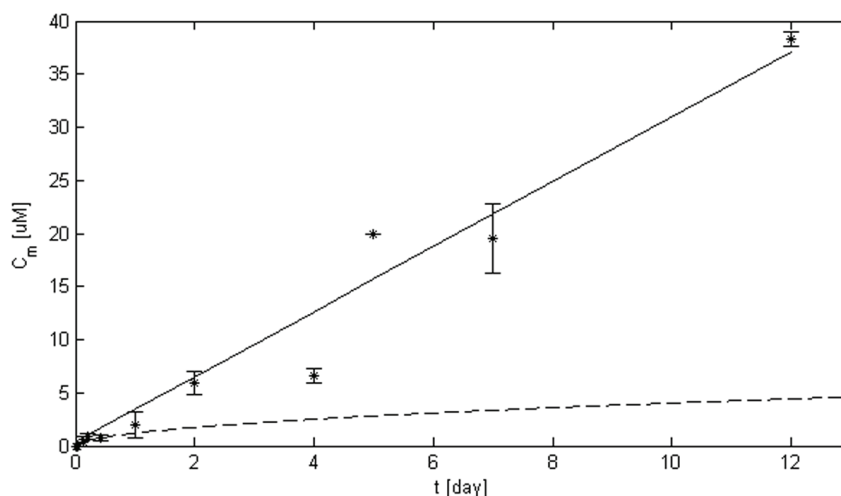

Figure 6. Released silver concentrations from the continuously perfused packed bed of Ag/alginate microbeads in water over time: experimental data (symbols), predictions of the internal diffusion model with $D_n = 6.9 \times 10^{-19}$ m^2 s^{-1} (dashed line) and predictions of the advection-diffusion model (solid line); data represent average of n = 3.
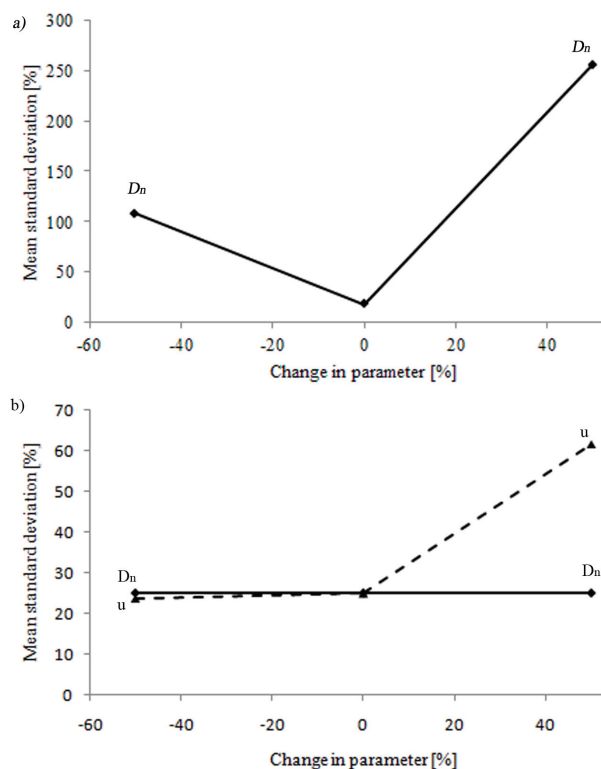
Figure 7. Sensitivity analysis. Mean standard deviations between modeling results and experimental data as functions of model parameters for silver release from Ag/alginate microbeads under: a) static conditions; b) perfusion.

DISCUSSION

In this study we have attempted to experimentally investigate and mathematically describe phenomena occurring during silver release from nanocomposite Ag/alginate hydrogels under conditions relevant for implantation in soft tissues. In specific, we have attempted to assess phenomena of AgNP/ion diffusion into a hydrogel imitating soft tissue at the implantation site as well as silver release into water under static and perfusion conditions relevant for hydrogel application at a non-vascularized and vascularized site, respectively. Two nanocomposite hydrogel forms were investigated in the present study (*i.e.*, discs and microbeads). Disc shape is directly related to the matrix-assisted autologous chondrocyte transplantation for treatment of cartilage defects. In this method, a biodegradable scaffold, which can be a membrane, mesh or a hydrogel, is seeded with autologous chondrocytes and implanted at the defect site after short-term cultivation [31]. It should be noted that treated cartilage lesions can range in size from 2–3 cm^2 up to 10 and 14 cm^2 [31]. On the other hand, microbead hydrogel form (< 1 mm in diameter) is already recognized for a long time as suitable for immobilization of different active substances and cells due to short diffusion distances (*e.g.*, [32]). Additionally, this form can be also suitable

as a cell scaffold in tissue engineering applications providing minimally invasive implantation by injection, structures enabling development of vasculature between individual particles, and consequently uniform regeneration of the extracellular matrix [33]. Thus, both investigated forms are related to development of soft tissue implants in which different strategies for incorporation and delivery of AgNPs can be envisioned. Due to high surface to volume ratio, microbeads will deliver AgNPs and/or ions at a faster rate than the discs, which, on the other hand, may serve as a reservoir of AgNPs. Indeed, silver diffusion from Ag/alginate discs into alginate hydrogels in direct contact was low and amounted to an average concentration in hydrogels of 39±6 µM (*i.e.* 4.1±0.6 µg Ag g^{-1} gel) during 14 days. In addition, this concentration corresponded to the initial bust release over the first day of experiment yielding the value of 35 µM, which was not further significantly increased. The released concentration corresponds to only 0.67% of the initial AgNP amount in Ag/alginate discs. Similar results were obtained in our previous studies of silver release from Ag/alginate microbeads in distilled water over 21 days amounting to ~1% of the initial silver content [24]. The observed low silver release is probably due to stability of electrochemically synthesized AgNPs, which were shown to be stabilized in alginate solutions by coordination with hydroxyl and ether groups, as well as by ring oxygen atoms in uronic acid residues in alginate molecules [13]. The released AgNPs/ions formed large clusters on the hydrogel surface and some smaller aggregates about 400 nm in size distributed within the hydrogel (Fig. 2b). This finding is in accordance with a previous report of deposition and uptake of AgNPs 20––50 nm in size by soybean roots [34]. The AgNPs formed amorphous aggregates on root surfaces ranging from a few µm to about 25 µm. Also, about 4.6% of AgNPs was internalized [34]. On the other hand, in an opposite experimental design of AgNP adsorption and/or absorption into methacrylate hydrogels from 0.5 mM and 1 mM AgNP dispersions, after 6 days of experiments total silver concentrations in hydrogels were similar as in the present work and in the range 10–14 µg Ag g^{-1} gel depending on the hydrogel cross-linking degree [35]. The authors proposed that AgNPs were mainly distributed on the outer hydrogel surfaces migrating deeper in the matrix as the adsorption time was prolonged [35]. However, stability of AgNPs and low silver release determined in the present study indicates potentials for use of Ag/alginate hydrogels as antimicrobial implants and coatings. This assumption is supported by the published results that stainless steel alloy implants with nanocomposite coatings consisting of AgNPs and poly(DL-lactic-co-glycolic acid) exhibited

antibacterial and osteoinductive properties both *in vitro* and *in vivo* in a rat femoral canal model [7].

Measurements of released silver concentrations in water from Ag/alginate microbeads under static conditions provided determination of the diffusion coefficient of AgNPs within Ag/alginate microbeads of 6.9×10^{-19} m^2 s^{-1}. This value is similar to that determined previously under static conditions for 4 nm AgNPs in Ag/alginate microbeads made of medium viscosity alginate amounting to 4.6×10^{-19} m^2 s^{-1} [24]. Slightly higher value obtained in the present work for fairly larger nanoparticles of 10–30 nm [13] is probably due to somewhat weaker hydrogel made of low viscosity alginate. However, in the presence of fluid flow AgNPs were washed out of the hydrogel with the interstitial fluid velocity estimated as 4.6 nm s^{-1}. Interestingly, in a previous study, silver release in the simulated body fluid from Ag/poly(*N*-vinyl-2-pyrrolidone) nanocomposite discs under static and prefusion conditions was insignificantly different indicating internal diffusion as the rate limiting step in both cases [36]. This result was attributed to fluid flow around hydrogel discs not affecting the silver release. On the contrary, in the present work, high specific surface area of microbeads and flow distribution through narrow channels of the packed bed evidently resulted in AgNP wash-out. The estimated low interstitial fluid velocity corresponds to low porosity of Ca-alginate hydrogels, which were reported to have a mesh size ranging from ~10 [37] to 20 nm [38]. However, even this low fluid flow induced significantly higher silver release as compared to static conditions (*i.e.*, 1 *vs*. 8%). This is especially important considering noticeably higher fluid velocities in the interstitium in the range of 0.1–4 μm s^{-1} [39]. Furthermore, mathematical modeling of quantum dot transport by convective diffusion from the epithelial barrier towards regional lymph nodes has indicated rate enhancement due to inflammation [40]. Thus, the effects of fluid flow determined in the present study are highly relevant for predicting the functionality of a potential Ag/alginate implant, which is dependent on the hydrodynamic properties of the implantation site.

CONCLUSION

In this study we have investigated phenomena occurring during AgNP transport from Ag/alginate hydrogels in water under conditions relevant for nanocomposite implantation. In the first experimental system we have investigated migration of AgNPs from the nanocomposite into the alginate hydrogel in direct contact mimicking soft tissue next to the implant. AgNPs were found to aggregate on the exposed hydrogel surface forming large clusters but also to penetrate into the hydrogel as smaller aggregates ~400 nm in size. Still the AgNP deposition was largely determined

by the initial burst release carried out over the first 24 h. After this period, silver concentration in the hydrogel stayed constant at ~39 μM corresponding to only 0.67% of the initial silver amount in the nanocomposite. These results indicated high stability of AgNPs within the Ag/alginate nanocomposite hydrogel implying potentials for use as antimicrobial implants and coatings. Similarly, Ag/alginate microbeads under static conditions in water released only 1% of the initial silver content over 21 days so that the AgNP diffusion coefficient within the microbeads was estimated as 6.9×10^{-19} m^2 s^{-1} However, under fluid flow as a model of a vascularized tissue site, nanocomposite Ag/alginate microbeads released 8% of the initial silver content over 12 days. A simple advection-diffusion model described well the experimental data indicating partial wash out of AgNPs from the microbeads by the interstitial fluid velocity estimated as 4.6 nm s^{-1}, which is significantly lower than reported fluid velocities in the interstitium. Thus, the results of the present study indicate the importance of careful design of the experimental set-up for *in vitro* evaluation of nanocomposites, which should closely resemble physiological settings in the envisioned application.

REFERENCES

[1] X.-F. Zhang, Z.-G. Liu, W. Shen, S. Gurunathan, Silver nanoparticles: synthesis, characterization, properties, applications, and therapeutic approaches, Int. J. Mol. Sci. **17** (2016) 1534–1568.

[2] H. Palza, Antimicrobial polymers with metal nanoparticles, Int. J. Mol. Sci. **16** (2015) 2099–2116.

[3] J. Natsuki, T. Natsuki, Y. Hashimoto, A review of silver nanoparticles: synthesis methods, properties and applications, Int. J. Mater. Sci. Appl. **4** (2015) 325–332.

[4] H. McVeigh, Topical silver for preventing wound infection, Int. J. Evid. Based. Healthc. **9** (2011) 454–455.

[5] B.S. Atiyeh, M. Costagliola, S.N. Hayek, S. Dibo, Effect of silver on burn wound infection control and healing: Review of the literature, Burns **33** (2007) 139–148.

[6] J. Stojkovska, Ž. Jovanović, I. Jančić, B. Bufan, M. Milenković, V. Mišković-Stanković, B Obradović, Novel Ag/alginate nanocomposites for wound treatments: animal studies, Rane **4** (2013) 17–22.

[7] Y. Liu, Z. Zheng, J.N. Zara, C. Hsu, D.E. Soofer, K.S. Lee , R.K. Siu , L.S. Miller, X. Zhang, D. Carpenter, C. Wang, K. Ting, C. Soo, The antimicrobial and osteoinductive properties of silver nanoparticle/poly (DL-lactic-co-glycolic acid)-coated stainless steel, Biomaterials **33** (2012) 8745–8756.

[8] W. Paul, C. Sharma, Chitosan and alginate wound dressings: a short review, Trends Biomater. Artif. Organs. **18** (2004) 18–23.

[9] K.Y. Lee, D.J. Mooney, Alginate: Properties and biomedical applications, Prog. Polym. Sci. **37** (2012) 106–126.

[10] E.A. Growney Kalaf, R. Flores, J.G. Bledsoe, S.A. Sell, Characterization of slow-gelling alginate hydrogels for intervertebral disc tissue-engineering applications, Mater. Sci. Eng. C **63** (2016) 198–210.

[11] J. Stojkovska, B. Bugarski, B. Obradovic, Evaluation of alginate hydrogels under *in vivo*-like bioreactor conditions for cartilage tissue engineering, J. Mater. Sci. Mater. Med. **21** (2010) 2869–2879.

[12] C.C. Wang, K.C. Yang, K.H. Lin, Y.L. Liu, H.C. Liu, F.H. Lin, Cartilage regeneration in SCID mice using a highly organized three-dimensional alginate scaffold, Biomaterials **33** (2012) 120–127.

[13] Ž. Jovanović, J. Stojkovska, B. Obradović, V. Miskovic-Stankovic, Alginate hydrogel microbeads incorporated with Ag nanoparticles obtained by electrochemical method, Mater. Chem. Phys. **133** (2012) 182–189.

[14] B. Obradovic, V. Mišković-Stanković, Ž. Jovanović, J. Stojkovska, 2015. Production of alginate microbeads with incorporated silver nanoparticles. patent RS53508 B1.

[15] M.C. Stensberg, Q. Wei, E.S. McLamore, D.M. Porterfield, A. Wei, M.S. Sepúlveda, Toxicological studies on silver nanoparticles: challenges and opportunities in assessment, monitoring and imaging, Nanomedicine (Lond). **6** (2011) 879–898.

[16] A.T. Florence, "Targeting" nanoparticles: The constraints of physical laws and physical barriers, J. Control. Release 1**64** (2012) 115–124.

[17] T.-Y. Lee, M.-S. Liu, L.-J. Huang, S.-I. Lue, L.-C. Lin, A.-L. Kwan, R.-C. Yang, Bioenergetic failure correlates with autophagy and apoptosis in rat liver following silver nanoparticle intraperitoneal administration, Part. Fibre Toxicol. **10** (2013) 40.

[18] B. Katsnelson, L.I. Privalova, V.B. Gurvich, O.H. Makeyev, V.Y. Shur, Y.B. Beikin, M.P. Sutunkova, E.P. Kireyeva, I. Minigalieva, N.V. Loginova, M.S. Vasilyeva, A.V. Korotkov, E. Shuman, L. Vlasova, E.V. Shishkina, A.E. Tyurnina, R.V. Kozin, I.E. Valamina, S.V. Pichugova, L.G. Tulakina, Comparative *in vivo* assessment of some adverse bioeffects of equidimensional gold and silver nanoparticles and the attenuation of nanosilver's effects with a complex of innocuous bioprotectors, Int. J. Mol. Sci. **14** (2013) 2449–2483.

[19] H.J. Johnston, G. Hutchison, F.M. Christensen, S. Peters, S. Hankin V. Stone, A review of the in vivo and *in vitro* toxicity of silver and gold particulates: particle attributes and biological mechanisms responsible for the observed toxicity, Crit. Rev. Toxicol. **40** (2010) 328–346.

[20] C. Rigo, L. Ferroni, I. Tocco, M. Roman, I. Munivrana, C. Gardin, W.R.L. Cairns, V. Vindigni, B. Azzena, C. Barbante, B.Zavan, Active silver nanoparticles for wound healing, Int. J. Mol. Sci. **14** (2013) 4817–4840.

[21] G. Doig, G.H. Yeoh, V. Timchenko, G. Rosengarten, T.J. Barber, S.C.P. Cheung, Simulation of blood flow and nanoparticle transport in a stenosed carotid bifurcation and pseudo-arteriole, J. Comput. Multiph. Flows **4** (2012) 85–102.

[22] A. Lankoff, W.J. Sandberg, A. Wegierek-Ciuk, H. Lisowska, M. Refsnes, B. Sartowska, P.E. Schwarze, S. Meczynska-Wielgosz, M. Wojewodzka, M. Kruszewski, The effect of agglomeration state of silver and titanium dioxide nanoparticles on cellular response of HepG2, A549 and THP-1 cells, Toxicol. Lett. **208** (2012) 197–213.

[23] H. Al-Obaidi, A.T. Florence, Nanoparticle delivery and particle diffusion in confined and complex environments, J. Drug Deliv. Sci. Technol. **30** (2015) 266–277.

[24] D. Kostic, S. Vidovic, B. Obradovic, Silver release from nanocomposite Ag/alginate hydrogels in the presence of chloride ions: experimental results and mathematical modeling, J. Nanoparticle Res. **18** (2016) 76–92.

[25] T.I. Klokk, J.E. Melvik., Controlling the size of alginate gel beads by use of a high electrostatic potential, J. Microencapsul. **19** (2002) 415–424.

[26] C. Rodríguez-Rivero, E.M.M. Del Valle, M.A. Galan, Experimental and linear analysis for the instability of non-Newtonian liquid jets issuing from a pressurized vibrating nozzle, AIChE J. **61** (2015) 2070–2078.

[27] C. Schwinger, A. Klemenz, K. Busse, J. Kressler, Encapsulation of living cells with polymeric systems, Macromol. Symp. **210** (2004) 493–499.

[28] U. Prusse, J. Dalluhn, J. Breford, K.-D. Vorlop, Production of spherical beads by JetCutting, Chem. Eng. Technol. **23** (2000) 1105–1110.

[29] J. Stojkovska, D. Kostić, Ž. Jovanović, M. Vukašinović-Sekulić, V. Mišković-Stanković, B. Obradović, A comprehensive approach to *in vitro* functional evaluation of Ag/alginate nanocomposite hydrogels, Carbohydr. Polym. **111** (2014) 305–314.

[30] N.M. Velings, M.M. Mestdagh, Physico-chemical properties of alginate gel beads, Polym. Gels Networks **3** (1995) 311–330.

[31] E. Kon, G. Filardo, B. Di Matteo, F. Perdisa, M. Marcacci, Matrix assisted autologous chondrocyte transplantation for cartilage treatment: A systematic review, Bone Joint Res. **2** (2013) 18–25.

[32] B. Bugarski, B. Obradovic, V.A. Nedovic, D. Poncelet, "Immobilization of cells and enzymes using electrostatic droplet generator", in Focus on Biotechnology, Volume 8a: Fundamentals of Cell Immobilisation Biotechnology, V. Nedovic, R.G. Willaert (Eds.), Kluwer Academic Publishers, Dordrecht, 2004, pp. 277–294.

[33] D.E. Orr, K.J. Burg, Design of a modular bioreactor to incorporate both perfusion flow and hydrostatic compression for tissue engineering applications, Ann. Biomed. Eng. **36** (2008) 1228–1241.

[34] B. Quah, C. Musante, J.C. White, X. Ma, Phytotoxicity, uptake, and accumulation of silver with different particle sizes and chemical forms, J. Nanoparticle Res. **17** (2015) 1–13.

[35] M.I. González-Sánchez, S. Perni, G. Tommasi, N.G. Morris, K. Hawkins, E. López-Cabarcos, P. Prokopovich, Silver nanoparticle based antibacterial methacrylate hydrogels potential for bone graft applications, Mater. Sci. Eng., C **50** (2015) 332–340.

[36] Z. Jovanovic, A. Radosavljevic, Z. Kacarevic-Popovic, J. Stojkovska, A. Peric-Grujic, M. Ristic, I.Z. Matic, Z.D. Juranic, B. Obradovic, V. Miskovic-Stankovic, Bioreactor validation and biocompatibility of Ag/poly(*N*-vinyl-2--pyrrolidone) hydrogel nanocomposites, Colloids Surfaces, B **105** (2013) 230–235.

[37] W.W. Stewart, H.E. Swaisgood, Characterization of calcium alginate pore diameter by size-exclusion chromatography using protein standards, Enzyme Microb. Technol. **15** (1993) 922–927.

[38] G. Fundueanu, C. Nastruzzi, A. Carpov, J. Desbrieres, M. Rinaudo, Physico-chemical characterization of Ca-alginate microparticles produced with different methods, Biomaterials **20** (1999) 1427–1435.

[39] J. Scallan, V.H. Huxley, R.J. Korthuis, Capillary Fluid Exchange: Regulation, Functions, and Pathology, Ch. 2, Morgan & Claypool Life Sciences, San Rafael, CA, 2010.

[40] S.S. Dukhin, M.E. Labib, Convective diffusion of nanoparticles from the epithelial barrier toward regional lymph nodes, Adv. Colloid Interface Sci. **199**–**200** (2013) 23–43.

IZVOD

TRANSPORT NANOČESTICA SREBRA IZ NANOKOMPOZITNIH Ag/ALGINATNIH HIDROGELOVA U USLOVIMA RELEVANTNIM ZA IMPLANTACIJU U TKIVA

Danijela D. Kostic[1], Ivana S. Malagurski[2], Bojana M. Obradovic[2]

[1]Inovacioni centar Tehnološko–metalurškog fakulteta, Karnegijeva 4, 11000 Beograd, Srbija
[2]Tehnološko–metalurški fakultet, Univerzitet u Beogradu, Karnegijeva 4, 11000 Beograd, Srbija

(Naučni rad)

Kako mikroorganizmi postaju sve otporniji na antibiotike, javlja se potreba za pronalaženjem novih rešenja za prevazilaženje ovog problema. Nanočestice srebra su pokazale izuzetnu antimikrobnu aktivnost, čak jaču od jonskog oblika ovog metala, a mogu se imobilisati unutar polimernih nosača čime se omogućava kontrolisano otpuštanje srebra i produženo dejstvo. Nanokompozitni hidrogelovi na bazi alginata su posebno atraktivni za biomedicinske primene usled svoje biokompatibilnosti, hidrofilnosti i velikog sorpcionog kapaciteta dok se inkorporisanjem nanočestica srebra omogućava i antimikrobna aktivnost. Međutim, primena nanokompozita u medicinske svrhe zahteva sveobuhvatna ispitivanja citotoksičnosti, genotoksičnosti, interakcija sa biološkim fluidima i kretanja i distribucije nanočestica u organizmu. Nanočestice se generalno mogu transportovati do različitih organa, tkiva i ćelija difuzijom ali i strujanjem krvi pri čemu su ovi procesi praćeni različitim kompleksnim pojavama kao što su agregacija, flokulacija i zadržavanje i adsorpcija nanočestica na pojedinim mestima. Cilj ovog rada je bio ispitivanje fenomena transporta nanočestica srebra iz nanokompozitnih Ag/alginatnih hidrogelova u uslovima koji su relevantni za potencijalnu biomedicinsku primenu kao implantata za meka tkiva. U prvoj eksperimentalnoj seriji ispitivana je migracija nanočestica srebra iz nanokompozita u alginatni hidrogel na koga nanokompozit direktno naleže što imitira implantat u dodiru sa mekim tkivom. Pokazalo se da je prenos nanočestica određen početnim otpuštanjem u toku 24 h tako da su se na površini hidrogela formirali veliki aglomerati nanočestica dok su u unutrašnjosti bili raspoređeni manji agregati prečnika oko 400 nm. Međutim, ukupno otpuštena količina srebra iz nanokompozita je bila mala (0.67%) što je ukazalo na stabilnost nanočestica u Ag/alginatnom hidrogelu. U sledećoj eksperimentalnoj seriji ispitivano je otpuštanje nanočestica srebra veličine 10-30 nm iz Ag/alginatnih mikročestica u statičkim uslovima, kao i pri kontinualnom protoku vode kroz pakovani sloj mikročestica površinskom brzinom od 100 μm s^{-1} što imitira uslove pri implantaciji u vaskularizovano tkivo. Eksperimentalni rezultati otpuštanja srebra u statičkim uslovima su dobro opisani modelom unutrašnje difuzije sa koeficijentom difuzije nanočestica u Ag/alginatnom hidrogelu od 6,9×10^{-19} m^2 s^{-1}. Sa druge strane, otpuštanje srebra pri kontinualnom protoku je bilo povećano tako da je razvijen i primenjen jednodimenzionalni model transporta nanočestica kroz hidrogel difuzijom i prenosom strujanjem unutar hidrogela. Pokazalo se da matematički model dobro opisuje eksperimentalne podatke sa vrednošću intersticijalne brzine od 4,6 nm s^{-1}. S obzirom na to da su brzine fluida u intersticijumu u organizmu značajno veće (0.1–4 μm s^{-1}) ovaj rezultat ukazuje na bitan uticaj hidrodinamičkih uslova na otpuštanje srebra i funkcionalnost potencijalnih implantata. Rezultati dobijeni u ovom radu upućuju da je za ispitivanje nanokompozita potrebno koncipirati eksperimentalne sisteme tako da obezbeđuju uslove što sličnije fiziološkim pri željenoj biomedicinskoj primeni.

Ključne reči: • Nanočestice srebra • agregacija • Konvektivni prenos • Matematičko modelovanje • Tkivni implantati